

Nutrient Stress Activates Inflammation and Reduces Glucose Metabolism by Suppressing AMP-Activated Protein Kinase in the Heart

Hwi Jin Ko,^{1,2} Zhiyou Zhang,² Dae Young Jung,^{1,2} John Y. Jun,^{2,3} Zhexi Ma,² Kelly E. Jones,² Sook Y. Chan,² and Jason K. Kim^{1,2,4}

OBJECTIVE—Heart failure is a major cause of mortality in diabetes and may be causally associated with altered metabolism. Recent reports indicate a role of inflammation in peripheral insulin resistance, but the impact of inflammation on cardiac metabolism is unknown. We investigated the effects of diet-induced obesity on cardiac inflammation and glucose metabolism in mice.

RESEARCH DESIGN AND METHODS—Male C57BL/6 mice were fed a high-fat diet (HFD) for 6 weeks, and heart samples were taken to measure insulin sensitivity, glucose metabolism, and inflammation. Heart samples were also examined following acute interleukin (IL)-6 or lipid infusion in C57BL/6 mice and in IL-6 knockout mice following an HFD.

RESULTS—Diet-induced obesity reduced cardiac glucose metabolism, GLUT, and AMP-activated protein kinase (AMPK) levels, and this was associated with increased levels of macrophages, toll-like receptor 4, suppressor of cytokine signaling 3 (SOCS3), and cytokines in heart. Acute physiological elevation of IL-6 suppressed glucose metabolism and caused insulin resistance by increasing SOCS3 and via SOCS3-mediated inhibition of insulin receptor substrate (IRS)-1 and possibly AMPK in heart. Diet-induced inflammation and defects in glucose metabolism were attenuated in IL-6 knockout mice, implicating the role of IL-6 in obesity-associated cardiac inflammation. Acute lipid infusion caused inflammation and raised local levels of macrophages, C-C motif chemokine receptor 2, SOCS3, and cytokines in heart. Lipid-induced cardiac inflammation suppressed AMPK, suggesting the role of lipid as a nutrient stress triggering inflammation.

CONCLUSIONS—Our findings that nutrient stress activates cardiac inflammation and that IL-6 suppresses myocardial glucose metabolism via inhibition of AMPK and IRS-1 underscore the important role of inflammation in the pathogenesis of diabetic heart. *Diabetes* 58:2536–2546, 2009

From the ¹Program in Molecular Medicine, University of Massachusetts Medical School, Worcester, Massachusetts; the ²Department of Cellular and Molecular Physiology, Pennsylvania State University College of Medicine, Hershey, Pennsylvania; the ³Department of Medicine, Division of Endocrinology, Diabetes and Metabolism, Pennsylvania State University College of Medicine, Hershey, Pennsylvania; and the ⁴Department of Medicine, Division of Endocrinology, Metabolism and Diabetes, University of Massachusetts Medical School, Worcester, Massachusetts.

Corresponding author: Jason K. Kim, jason.kim@umassmed.edu.

Received 3 October 2008 and accepted 2 August 2009. Published ahead of print at <http://diabetes.diabetesjournals.org> on 18 August 2009. DOI: 10.2337/db08-1361.

H.J.K. and Z.Z. contributed equally to this article and should be considered co-first authors.

© 2009 by the American Diabetes Association. Readers may use this article as long as the work is properly cited, the use is educational and not for profit, and the work is not altered. See <http://creativecommons.org/licenses/by-nc-nd/3.0/> for details.

The costs of publication of this article were defrayed in part by the payment of page charges. This article must therefore be hereby marked "advertisement" in accordance with 18 U.S.C. Section 1734 solely to indicate this fact.

Type 2 diabetes is the most common metabolic disease in the world, affecting >250 million people, and cardiovascular disease is the leading cause of mortality in diabetes (1). Although the underlying mechanism by which diabetes increases cardiovascular events is unknown, perturbations in cardiac metabolism are among the earliest diabetes-induced alterations in the myocardium, preceding both functional and pathological changes, and may play a causative role in diabetic heart failure (2,3). Studies using isolated perfused-heart preparations, cultured cardiomyocytes, and positron emission tomography uniformly showed insulin resistance in human and animal models of diabetic heart (4,5). Diabetic heart is also characterized with elevated lipid oxidation with reciprocal reduction in glucose metabolism (6). Our recent study (7) found that chronic high-fat feeding impairs myocardial glucose metabolism, and this was associated with ventricular hypertrophy and cardiac dysfunction in obese mice. These findings highlight the importance of understanding the mechanism by which obesity and diabetes affect cardiac metabolism.

Increasing evidence indicates the role of chronic inflammation and macrophage activation in insulin resistance (8,9). A cohort of recent studies (10–13) demonstrated increases in macrophage infiltration and cytokine expression in adipose tissue and their association with insulin resistance in obese humans and animal models. Tumor necrosis factor (TNF)- α is a proinflammatory cytokine that is secreted by macrophages and adipocytes and is shown to cause insulin resistance by inhibiting insulin signaling, AMP-activated protein kinase (AMPK), and the glucose transport system (14,15). Interleukin (IL)-6 is another proinflammatory cytokine that is elevated in obese diabetic subjects and is shown to cause insulin resistance by activating STAT3-suppressor of cytokine signaling 3 (SOCS3) expression and inhibiting the insulin signaling pathway in liver and adipose tissue (16–18). However, the role of IL-6 in insulin resistance remains debatable largely due to its differential effects on glucose metabolism in skeletal muscle, adipose tissue, and liver (19). Despite the wealth of information on the role of inflammation in peripheral insulin resistance, the impact of inflammation on cardiac metabolism has not been previously addressed. In this article, we demonstrate that diet-induced obesity increases macrophage and cytokine levels in heart. IL-6 reduces glucose metabolism by suppressing AMPK and insulin receptor substrate (IRS)-associated insulin signaling in heart, whereas IL-6-deficient mice are protected from diet-induced alterations in glucose metabolism. The fact that acute lipid infusion increases the inflammatory

response and impairs myocardial glucose metabolism, similar to the effects of high-fat feeding, suggests the role of nutrient stress in the activation of toll-like receptor (TLR) 4 signaling and inflammation in heart. Since glucose is an important source of energy for a working heart, particularly during ischemia, our findings identify an important role of inflammation in the pathogenesis of diabetic heart failure.

RESEARCH DESIGN AND METHODS

Animals and high-fat feeding. Male C57BL/6 mice at ~10 weeks of age were obtained from The Jackson Laboratory and housed under controlled temperature and lighting (0700–1900 light cycle, 1900–0700 dark cycle) with free access to food and water. Mice were fed a high-fat diet (HFD) (55% fat by calories; Harlan Teklad TD93075, Madison, WI) or standard diet (Harlan Teklad LM-485) ad libitum for 6 weeks ($n = 5-7$). IL-6-deficient (IL-6 knockout [KO]) breeder mice (C57BL/6 background) were obtained from The Jackson Laboratory, and IL-6 KO mice have been bred to form colonies. Immediately after weaning (~4 weeks of age), male IL-6 KO mice and wild-type littermates were fed standard diet or HFD for 3 weeks ($n = 6-7$). Additional male C57BL/6 mice were used for the acute IL-6 infusion and lipid infusion studies. Whole-body fat and lean mass were noninvasively measured in conscious mice using proton magnetic resonance spectroscopy ($^1\text{H-MRS}$) (Echo Medical Systems, Houston, TX). All procedures were approved by the institutional animal care and use committee of the University of Massachusetts Medical School and the Pennsylvania State University College of Medicine.

Metabolic studies to measure myocardial glucose metabolism. At 4–5 days before the metabolic experiments, mice were anesthetized, and an indwelling catheter was inserted in the right internal jugular vein. Following overnight fast (~15 h), basal myocardial glucose uptake was measured using an intravenous injection of 2-deoxy-D-[1- ^{14}C]glucose (2-[^{14}C]DG; 10 μCi) (PerkinElmer, Boston, MA) in conscious mice. Following injection, blood samples were taken at 5-min intervals for 30 min for the measurement of plasma 2-[^{14}C]DG concentrations. At the end of experiments, mice were anesthetized and heart samples were collected for analysis (20).

For the assessment of myocardial insulin sensitivity, a 2-h hyperinsulinemic-euglycemic clamp was conducted with a primed (150 mU/kg body wt) and continuous infusion of human regular insulin (Humulin; Eli Lilly, Indianapolis, IN) at a rate of 2.5 mU \cdot kg $^{-1}$ \cdot min $^{-1}$ to raise plasma insulin within a physiological range (21). Blood samples (20 μl) were collected at 20-min intervals for the immediate measurement of plasma glucose concentration, and 20% glucose was infused at variable rates to maintain glucose at basal concentrations. To estimate insulin-stimulated glucose uptake in individual organs, 2-[^{14}C]DG was administered as a bolus (10 μCi) at 75 min after the start of clamps. Blood samples were taken before, during, and at the end of clamps for the measurement of plasma [^3H]glucose, $^3\text{H}_2\text{O}$, 2-[^{14}C]DG concentrations, and/or insulin concentrations. At the end of the clamps, mice were anesthetized and tissues were taken for biochemical and molecular analysis (21).

Biochemical assays. Glucose concentrations during clamps were analyzed using 10 μl plasma by a glucose oxidase method on Analox GM9 Analyser (Analox Instruments, Hammersmith, London, U.K.). Plasma free fatty acid (FFA) concentrations were measured using Sigma diagnostic kits (Sigma Diagnostics, St. Louis, MO) and spectrophotometry. Plasma IL-6 and TNF- α levels were determined using enzyme-linked immunosorbent assays. Plasma concentrations of [^3H]glucose, 2-[^{14}C]DG, and $^3\text{H}_2\text{O}$ were determined following deproteinization of plasma samples as previously described (21). For the determination of tissue 2-[^{14}C]DG-6-P content, tissue samples were homogenized, and the supernatants were subjected to an ion-exchange column to separate 2-[^{14}C]DG-6-P from 2-[^{14}C]DG. Basal and insulin-stimulated glucose uptake in individual tissues was assessed by determining the tissue content of 2-[^{14}C]DG-6-P and plasma 2-[^{14}C]DG profile. We acknowledge that 2-[^{14}C]DG is used to measure glucose uptake into cells, but it does not directly assess glucose transport versus glucose phosphorylation steps.

Acute IL-6 infusion study. Following an overnight fast, mouse recombinant IL-6 (16 ng/h; Sigma) or saline (matched volume; control) was continuously infused for 4 h in order to cause an acute physiological elevation of IL-6. Metabolic studies were performed toward the end of IL-6 or saline infusion, and heart samples were collected for analysis.

Acute lipid infusion study. Following an overnight fast, lipids (2.5 ml \cdot kg $^{-1}$ \cdot h $^{-1}$, triglyceride emulsion) and heparin (6 units/h) or glycerol (matching volume; control) were continuously infused for 5 h to raise plasma fatty acid levels in male C57BL/6 mice ($n = 10-11$ for each group). Before and at the end of the 5-h infusion, blood samples were taken for the measurement of plasma

FFA concentrations. At the end of the experiment, mice were anesthetized and heart samples were collected for analysis.

Molecular analysis for inflammatory signaling. Heart samples were obtained at the basal state for the following analysis. STAT3 protein expression and tyrosine phosphorylation were measured in heart using STAT3 phospho-Tyr 705 antibody (1:1,000 dilution; Cell Signaling Technology, Danvers, MA). For heart levels of CD68, C-C motif chemokine receptor (CCR)-2, SOCS3, TLR4, and MyD88, heart tissues (50 mg) were grounded, and powdered tissues were lysed in 800 μl of ice-cold lysis buffer containing protease inhibitor cocktail and 1% Triton X-100. Tissue lysates were sonicated, incubated, and centrifuged for 40 min. A total of 100 μg of each protein were mixed with sample loading buffer (2 \times concentration) and loaded in 10% gel. Proteins resolved by SDS-PAGE were transferred to nitrocellulose membrane. The membrane was blocked and incubated with polyclonal antibodies for CD68, CCR2, SOCS3 (Santa Cruz Biotechnology, Santa Cruz, CA), TLR4 (Cell Signaling Technology), and MyD88 (Millipore, Billerica, MA). The membrane was washed and incubated with the horseradish peroxidase-conjugated secondary antibody (Bio-Rad Laboratories, Hercules, CA) in 1% BSA in Tris-buffered saline Tween 20 (TBST) (50 mmol/l Tris-HCl, pH 7.5, 100 mmol/l NaCl, 0.1% Tween 20) for 1 h at room temperature. Detection of immunoreactive bands were achieved and quantified.

Co-immunoprecipitation assay. A total of 50 mg of heart tissue were lysed and prepared as described. A total of 20 μl of protein A sepharose CL-4B beads (Amersham Biosciences, Uppsala, Sweden) per reaction were equilibrated with 500 μl of lysis buffer for 15 min, centrifuged, and supernatants removed. A total of 10 μl of the equilibrated beads were added to the extract to preclear extract. This mixed extract was incubated for 20 min and centrifuged, and the precleared extract was transferred. A total of 20 μl of the equilibrated beads per reaction were added to the lysis buffer. Each 2 μg of antibody (phospho-AMPK α , AMPK α , or SOCS3) was added and incubated for 1 h. After centrifuge, supernatant was removed. Antibody-coupled beads were dispensed into tubes, and protein extracts were added and incubated at 4 $^{\circ}\text{C}$ overnight. The solution was washed five times using lysis buffer. In the final wash, supernatant was removed. A total of 50 μl of sample loading buffer (2 \times concentration) was added and boiled at 95 $^{\circ}\text{C}$ for 3 min. The tube was shaken for 5 min to ensure the release of most immunoprecipitated proteins and centrifuged. Precipitated proteins were loaded in 10% gel for SDS-PAGE. Proteins resolved by SDS-PAGE were transferred to nitrocellulose membrane. The membranes were blocked with 5% BSA in TBST for 1 h and incubated with phospho-AMPK α , AMPK α , and SOCS3 antibody in 1% BSA in TBST overnight at 4 $^{\circ}\text{C}$. Immunoreactive bands were detected.

Molecular analysis of metabolic signaling. For IRS-1 tyrosine phosphorylation, heart samples were obtained at the end of euglycemic clamps to measure in vivo insulin signaling activity. Immunoblotting was performed using powdered heart tissue samples dissolved in lysis buffer (50 mmol/l HEPES, pH 7.3, 137 mmol/l NaCl, 1 mmol/l MgCl $_2$, 1 mmol/l CaCl $_2$, 2 mmol/l NaVO $_4$, 10 mmol/l sodium pyrophosphate, 10 mmol/l NaF, 2 mmol/l EDTA, 2 mmol/l PMSF, 10 mmol/l benzamide, 10% glycerol, 1% Triton X-100, 1 mmol/l microcystin LR, and 100 nmol/l Okadaic acid) (Sigma-Aldrich, St. Louis, MO) and cocktail protease inhibitor (Roche Diagnostic, Mannheim, Germany) and sonicated for 10 s. The samples were incubated on ice for 30 min, centrifuged at 15,000g for 15 min at 4 $^{\circ}\text{C}$, and the supernatants harvested. Protein concentrations were determined using the Bio-Rad DC protein assay (Bio-Rad Laboratories). Immunoprecipitation was performed with 3 mg total protein and 4 μg anti-IRS-1 antibodies (Upstate Biotechnology, Lake Placid, NY), rotating overnight at 4 $^{\circ}\text{C}$. IRS-1 and anti-IRS-1 antibody complex was pulled down by protein A-sepharose CL-4B beads (Amersham Biosciences, Uppsala, Sweden), and the beads were rinsed three times in PBS. Gel sample buffer was added, boiled for 10 min, and loaded onto SDS gels. Western blot was performed, and the membranes were blocked by incubation in 5% BSA in TBST and then incubated in anti-phosphotyrosine antibodies (1:1,000 dilution; Upstate Biotechnology, Charlottesville, VA) overnight at 4 $^{\circ}\text{C}$. Membranes were then stripped to be reprobed by anti-IRS-1 antibodies. For AMPK phosphorylation and total protein levels, heart samples were obtained in the basal state, and immunoblotting was performed using antibodies against AMPK α and phospho-Thr 172 AMPK α (Cell Signaling Technology).

Immunohistochemistry assay. Heart samples were fixed for 24 h at room temperature in Bouin's solution (Sigma-Aldrich), and the samples were placed into cassettes, which were immersed in 70% EtOH. A total of 70% EtOH was changed several times to wash away the fixative until it became clear. Heart tissue was embedded in paraffin. Tissue sections (5 μm) were mounted on charged glass slides. For deparaffinizing tissue, a slide was incubated for 5 min in clean xylene, 100% EtOH, 95% EtOH, 85% EtOH, 70% EtOH, and ultrapure water. Tissue section was immersed in Tris-EDTA buffer (10 mmol/l Tris, 1 mmol/l EDTA, 0.05% Tween 20, pH 9.0) (Sigma-Aldrich) at 95 $^{\circ}\text{C}$ for 20 min to retrieve antigen and cooled at room temperature for 20 min. Tissue sections were rinsed with TBST for 5 min two times, blocked in TBST (20 mmol/l Tris,

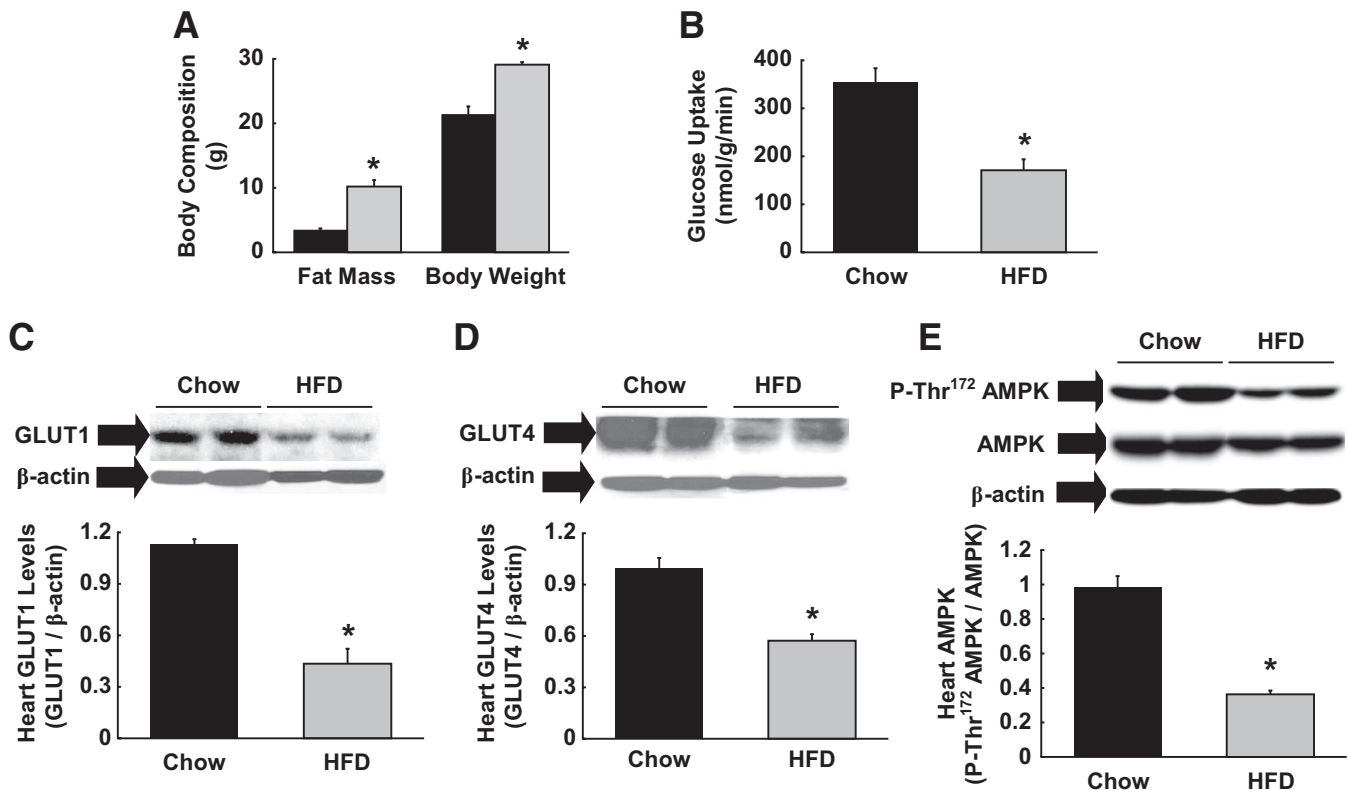


FIG. 1. High-fat feeding reduces glucose metabolism in heart. Male C57BL/6 mice were fed a HFD or standard (chow) diet for 6 weeks, and heart samples were taken at the end. **A:** Whole-body fat mass measured using ^1H -MRS and body weight were increased following 6 weeks of HFD. ■, Standard diet; □, HFD. **B:** Basal rate of myocardial glucose uptake, measured using 2- ^{14}C]deoxyglucose injection, was reduced following HFD. **C:** Total GLUT1 protein levels in heart were reduced in HFD-fed mice. **D:** Total GLUT4 protein levels. **E:** Thr¹⁷²-phosphorylation of AMPK normalized to total AMPK protein levels in heart was reduced following HFD. Values are means \pm SE for five to seven mice in each experiment. * $P < 0.05$ vs. standard diet-fed mice.

137 mmol/l NaCl, 0.05% Tween 20, pH 7.5) containing 10% BSA at room temperature for 40 min, and incubated in TBST containing anti-CD68 antibody at room temperature for 2 h. Tissue slide was washed for 5 min with TBST three times. A horseradish peroxidase-conjugated secondary antibody (Bio-Rad) was used for staining at room temperature for 1 h. After washing three times, metal-enhanced 3,3'-diaminobenzidine substrate was added to tissue and incubated for 15 min. Tissue was also counterstained with hematoxylin stain for 1 min, washed with ultrapure water, and mounted with mounting media (Thermo Fisher Scientific, Waltham, MA).

Immunofluorescence assay. Briefly, heart tissue sections were fixed in acetone/methanol (1:3) for 10 min and washed with PBS Tween 20 (PBST) (10 mmol/l sodium phosphate, 150 mmol/l sodium chloride, 0.3% Tween 20, pH 7.8) two times. Tissue sections were blocked in PBST containing 5% goat serum for 1 h at room temperature and washed with PBST two times. For immunostaining of cardiomyocyte and SOCS3, monoclonal cardiac troponin T and SOCS3 antibodies were used. For STAT3, phospho-STAT3 (Tyr⁷⁰⁵) and STAT3 antibodies (Cell Signaling Technology) were used. An anti-rabbit IgG fluorescein isothiocyanate and anti-mouse IgG tetramethylrhodamine isothiocyanate (Sigma-Aldrich) were used as a secondary antibody. Seventy, 80, and 100% ethanol were used each for 1 min for dehydration, and tissue sections were dried by air. Nuclei were stained with 4',6'-diamidino-2-phenylindole (VECTA Laboratories, Burlingame, CA). Fluorescence was analyzed using a fluorescence microscope.

Statistical analysis. Data are expressed as means \pm SE. The significance of the difference in mean values was evaluated using the Student's *t* test. The statistical significance was at the $P < 0.05$ level.

RESULTS

Effects of diet-induced obesity on cardiac metabolism. Male C57BL/6 mice were fed an HFD or standard diet for 6 weeks. High-fat feeding increased body weight and caused a threefold increase in whole-body fat mass, measured using ^1H -MRS, in mice (Fig. 1A). Myocardial glucose metabolism was measured using an intravenous injection

of 2- ^{14}C]DG in conscious mice. Basal myocardial glucose uptake was significantly reduced in HFD-fed mice (Fig. 1B), and this was associated with $\sim 60\%$ reductions in myocardial levels of total GLUT1 and GLUT4, the major glucose transporters in cardiomyocytes (Fig. 1C and D). These results are consistent with previous observations of reduced myocardial glucose metabolism in obese humans and animal models (5,22). AMPK is an important regulator of cardiac metabolism (23), and Thr¹⁷² phosphorylation of AMPK was markedly reduced in the heart following HFD (Fig. 1E). Total AMPK protein levels in heart tended to be lower following HFD. These data indicate that diet-induced reductions in glucose metabolism may be due to blunted AMPK levels in heart.

Diet-induced obesity induces inflammation in heart. Consistent with the previous observation of increased inflammatory cytokines in obese humans (16), plasma IL-6 and TNF- α levels were significantly elevated in HFD-fed mice (Fig. 2A). We also measured myocardial cytokine levels following HFD. Local IL-6 levels in heart were increased by 40% in HFD-fed mice (0.45 ± 0.02 vs. 0.32 ± 0.03 pg/100 μg in standard diet heart; $P < 0.05$). Local TNF- α levels tended to increase in the HFD heart, but this difference did not reach statistical significance (data not shown). These data indicate that while elevated serum cytokine levels following HFD are largely contributed by peripheral organs, such as adipose tissue, increased cytokine levels in heart may be partly due to local production either from cardiomyocytes or infiltrating macrophages. Interestingly, a modest systemic inflammation was associ-

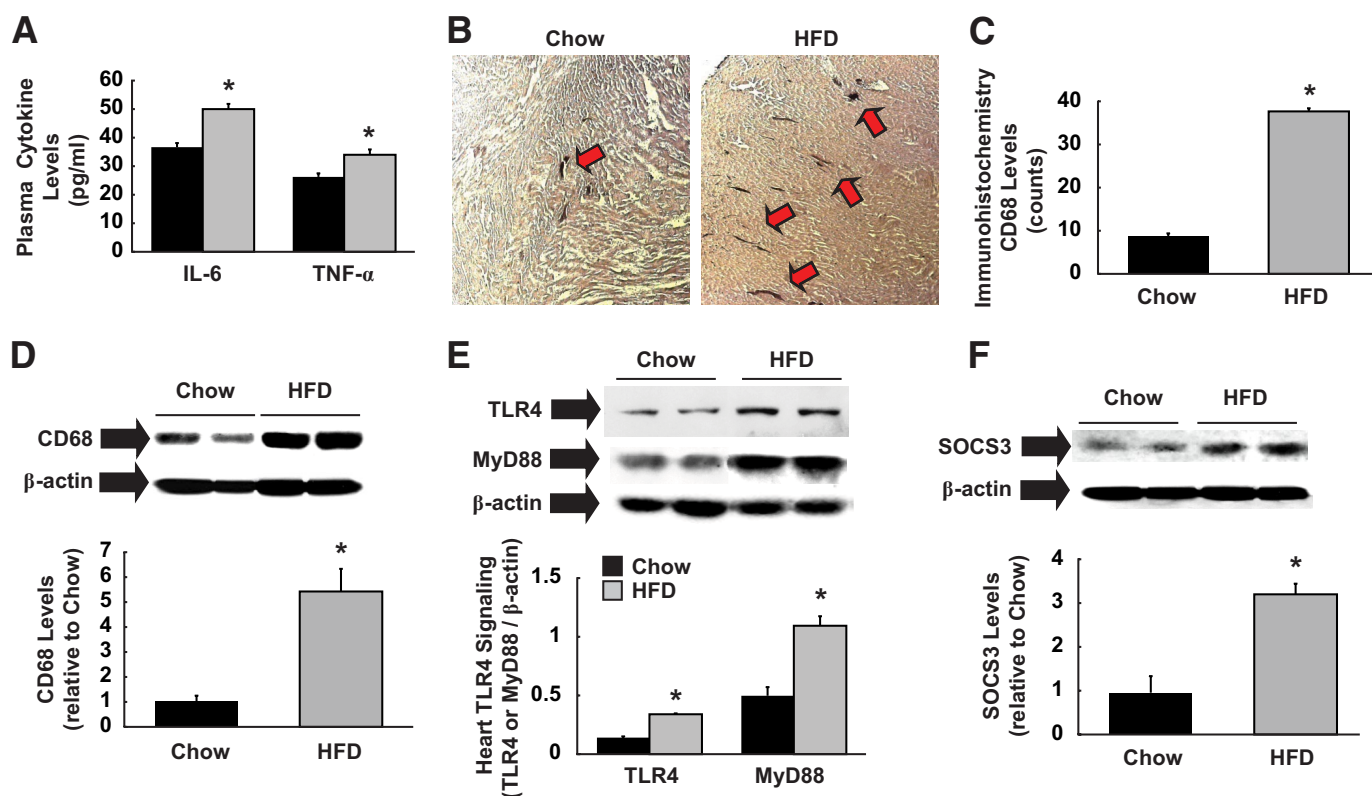


FIG. 2. High-fat feeding induces inflammation in heart. **A:** Plasma IL-6 and TNF- α levels were elevated in HFD-fed mice. ■, Standard diet; □, HFD. **B:** Immunohistochemistry using anti-CD68 of heart samples obtained after HFD or standard (chow) diet. CD68 markers, shown with red arrows, are elevated in HFD heart. **C:** Quantification of immunohistochemical CD68 levels. **D:** Macrophage-specific CD68 protein levels normalized to β -actin in heart was elevated in HFD-fed mice. **E:** TLR4 and MyD88 expression normalized to β -actin were elevated in HFD heart. **F:** SOCS3 protein levels normalized to β -actin were increased in heart following HFD. Values are means \pm SE for five to seven mice in each experiment. * $P < 0.05$ vs. standard diet-fed mice. (A high-quality color digital representation of this figure is available in the online issue.)

ated with an approximately four- to fivefold increase in macrophage levels (CD68 as a marker) in heart following HFD (Fig. 2B–D). Although macrophage infiltration in adipose tissue was previously observed in obese humans and animal models (8), to our knowledge, this is the first demonstration of increased macrophage levels in the heart of modestly obese animals. TLR4 was recently shown to regulate obesity-associated inflammation (24,25). After 6 weeks of HFD, TLR4 and MyD88 expression levels were increased by threefold (Fig. 2E), suggesting the role of TLR4 signaling in diet-induced inflammation in heart. Additionally, myocardial levels of SOCS3, which is synthesized in response to cytokine stimulation, were elevated in HFD-fed mice (Fig. 2F). To determine whether SOCS3 is increased within the cardiomyocytes, we performed immunofluorescence staining using antibodies to cardiomyocyte-specific troponin T and SOCS3. Our data indicate that HFD induced a notable increase in SOCS3 immunofluorescence staining that overlapped with troponin T fluorescence, suggesting cardiomyocyte elevation of SOCS3 following HFD (Fig. 3). Taken together, these results indicate that modest obesity induced by HFD causes inflammation by increasing TLR4 and local macrophage levels in heart. Elevated cytokines, such as IL-6 and TNF- α , increase intracellular SOCS3 levels and downregulate myocardial glucose metabolism by suppressing AMPK and GLUT1 and -4 protein levels, similar to their effects in peripheral organs (21,26).

Effects of acute IL-6 infusion on cardiac metabolism. To further examine the role of inflammatory cytokines in modulating myocardial metabolism, a physiological dose

of mouse recombinant IL-6 (16 ng/h) or saline (control) was intravenously infused for 4 h in conscious C57BL/6 mice. Such IL-6 dose was previously shown to elevate plasma IL-6 levels to approximately fourfold above basal, which approximates the levels found in obese subjects (16,26,27). Tyr⁷⁰⁵ phosphorylation of STAT3 was increased by twofold following IL-6 infusion, demonstrating IL-6 stimulation of heart (Fig. 4A). IL-6 infusion caused a 40% reduction in basal myocardial glucose uptake, which resembled the effects of HFD (Fig. 4B). We performed a 2-h hyperinsulinemic-euglycemic clamp to assess cardiac insulin action in conscious mice (21). IL-6 infusion reduced insulin-stimulated heart glucose uptake by \sim 50% as compared with the controls (Fig. 4C), and this was associated with profound reductions in total AMPK protein and AMPK phosphorylation (Thr¹⁷²) levels in heart (Fig. 4D and E). The ratio of phospho-AMPK to AMPK was further reduced in IL-6-treated heart (0.23 ± 0.06 vs. 1.17 ± 0.43 in controls). These data suggest that IL-6 downregulates myocardial glucose metabolism by suppressing AMPK, and this is consistent with the inhibitory effects of TNF- α on AMPK signaling in skeletal muscle (15). Additionally, IL-6 infusion reduced insulin-stimulated tyrosine phosphorylation of IRS-1, a key insulin signaling protein in heart (Fig. 4F).

IL-6 causes cardiac inflammation and suppresses AMPK. We next determined whether a systemic increase in IL-6 level causes local inflammation in heart. Similar to the effects of HFD, IL-6 infusion increased local macrophage levels in heart (Fig. 5A). Although this increase was statistically significant, it was less remarkable than the

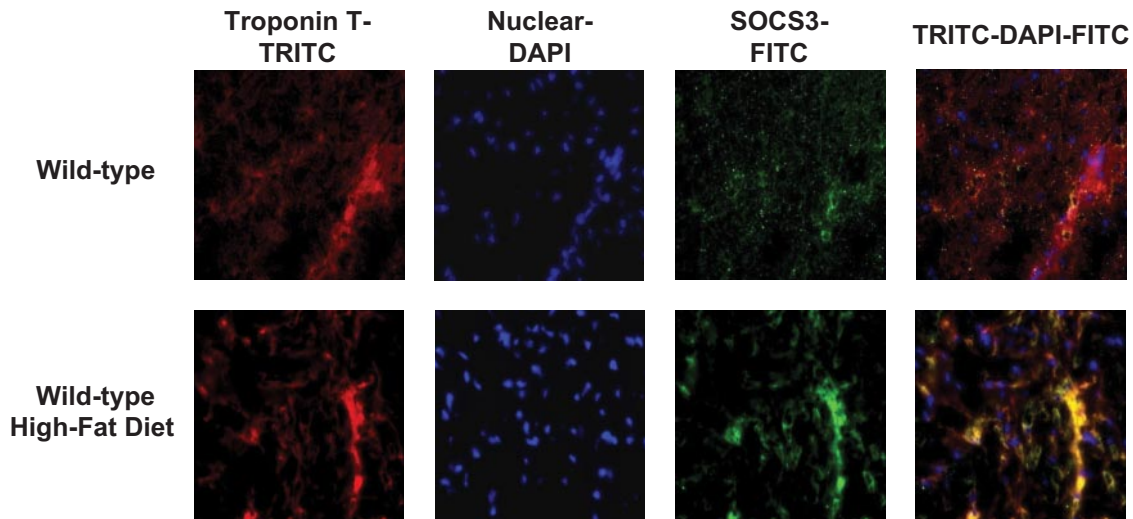


FIG. 3. Immunofluorescence staining using cardiomyocyte-specific troponin T-tetramethyl rhodamine isothiocyanate (TRITC) (red), nuclear 4',6-diamidino-2-phenylindole (DAPI) (blue), SOCS3-fluorescein isothiocyanate (FITC) (green), and combined TRITC-DAPI-FITC. Yellow coloration in combined staining indicates intense overlap staining of red TRITC-troponin T and green FITC-SOCS3. (A high-quality color digital representation of this figure is available in the online issue.)

effects of HFD, suggesting that other cytokines, such as TNF- α , likely contribute to the diet-induced cardiac inflammation. Myocardial SOCS3 levels following IL-6 infusion were markedly elevated (Fig. 5B), suggesting that SOCS3 may be involved in IL-6-mediated downregulation of insulin signaling in heart. Previously observed interaction between SOCS3 and IRS-1 raises the possibility that SOCS3 may interact with AMPK. To test this hypothesis,

we performed a coimmunoprecipitation assay using antibodies against AMPK α and SOCS3. Here, we report that SOCS3 was detected in AMPK and pAMPK immunoprecipitates (Fig. 5C). To the best of our knowledge, this is the first demonstration of interaction between SOCS3 and AMPK and supports the notion that SOCS3-induced targeting of AMPK to ubiquitin-mediated degradation, as shown to occur with IRS-1, may be responsible for reduced total

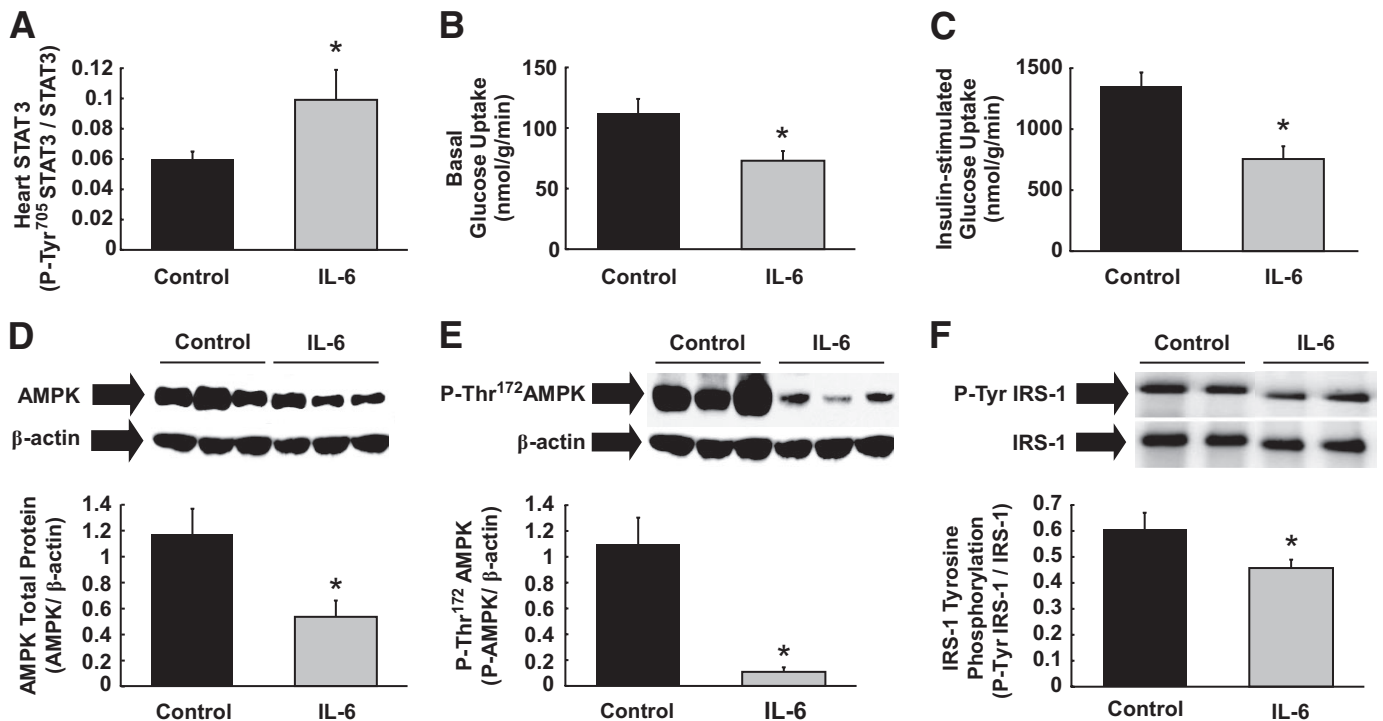


FIG. 4. Acute physiological elevation of IL-6 reduces myocardial glucose metabolism by suppressing AMPK and IRS-1. Mouse recombinant IL-6 or saline (control) was intravenously infused into C57BL/6 mice for 4 h, and heart samples were taken for analysis. **A:** Tyr⁷⁰⁵-phosphorylation of STAT3 normalized to total STAT3 protein level was increased in heart following IL-6 infusion. **B:** Basal myocardial glucose uptake was reduced following IL-6 infusion. **C:** A 2-h hyperinsulinemic-euglycemic clamp was performed during the final 2 h of IL-6 or saline infusion in C57BL/6 mice. Acute IL-6 infusion reduced insulin-stimulated glucose uptake in heart. **D:** Total AMPK protein levels normalized to β -actin were reduced in the heart of IL-6 infused mice. **E:** IL-6 infusion reduced Thr¹⁷²-phosphorylation of AMPK normalized to β -actin in heart. **F:** Insulin-stimulated tyrosine phosphorylation of IRS-1 normalized to IRS-1 protein levels in heart was reduced following IL-6 infusion. Values are means \pm SE for six to eight mice in each experiment. * $P < 0.05$ vs. control.

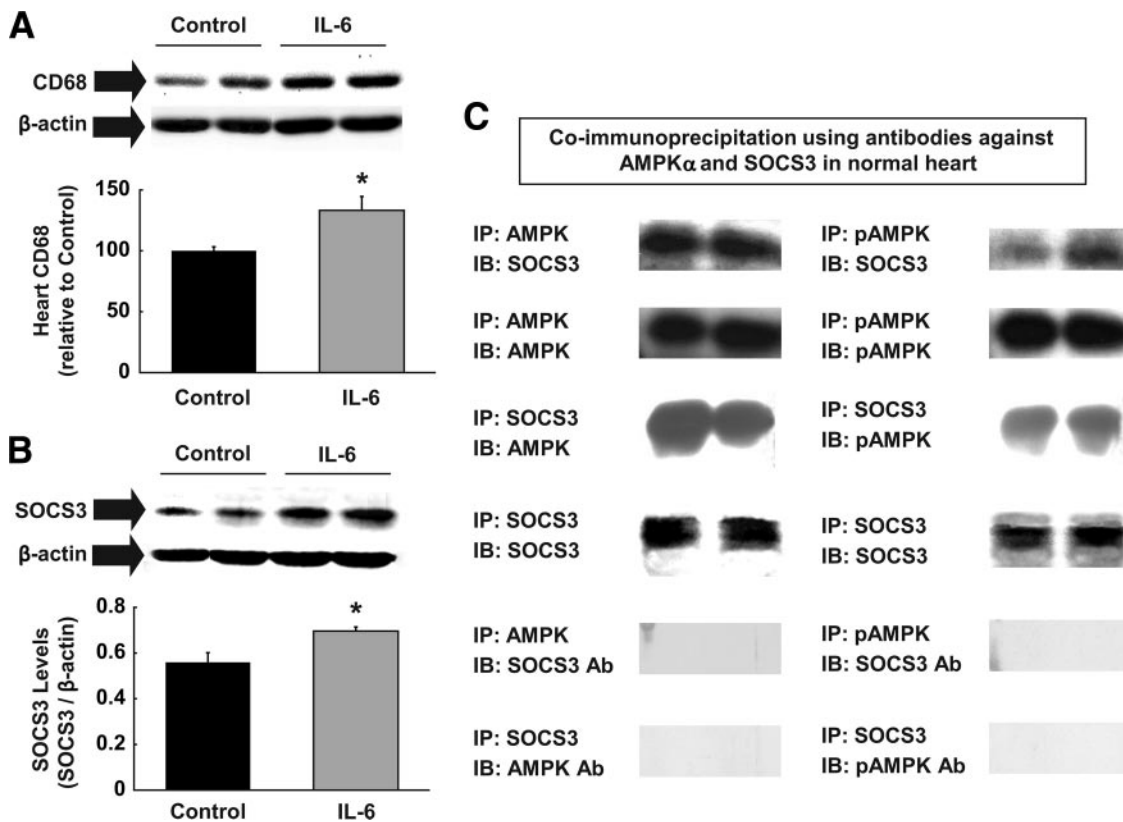


FIG. 5. Acute IL-6 infusion stimulates inflammatory response in heart. **A:** Macrophage-specific CD68 levels normalized to β -actin were elevated in heart following IL-6 infusion. **B:** SOCS3 protein levels normalized to β -actin were increased in IL-6-infused heart. **C:** We performed coimmunoprecipitation assay using antibodies to phospho-AMPK α , AMPK α , and SOCS3 in heart samples obtained from C57BL/6 mice. SOCS3 antibody pulled down both AMPK and phospho-AMPK, and AMPK antibody pulled down SOCS3 in normal heart, indicating the direct interaction between SOCS3 and AMPK. Immunoprecipitation of AMPK (or phospho-AMPK) and immunoblotting the AMPK-targeted site with SOCS3 antibody or immunoprecipitation of SOCS3 and immunoblotting the SOCS3 targeted site with AMPK (or phospho-AMPK) were used as negative controls. Values are means \pm SE for four to five mice in each experiment. * $P < 0.05$ vs. control.

AMPK protein levels in IL-6-treated heart. Alternatively, IL-6 infusion may reduce the cardiomyocyte synthesis of AMPK, resulting in lower levels of total AMPK. Thus, these results indicate that IL-6, at least partly, contributes to diet-induced inflammation in heart and downregulates glucose metabolism by increasing SOCS3 and SOCS3-mediated suppression of IRS-1 and possibly AMPK in heart.

Diet-induced cardiac insulin resistance and inflammation are attenuated in IL-6-deficient mice. To further determine the role of IL-6, the effects of HFD on cardiac metabolism were determined in IL-6 KO mice. HFD was fed in both groups of mice shortly after weaning (~4 weeks of age) in order to match diet-induced adiposity in these mice. Following 3 weeks of HFD, whole-body fat mass was similarly increased in IL-6 KO and wild-type mice (Fig. 6A). Whole-body lean mass was comparable between the groups, suggesting a similar growth pattern in these mice during HFD (Fig. 6B). A 2-h hyperinsulinemic-euglycemic clamp was performed in IL-6 KO and wild-type mice following HFD. HFD reduced insulin-stimulated heart glucose uptake in wild-type mice, but IL-6 KO mice were protected from diet-induced myocardial insulin resistance (Fig. 6C). Myocardial AMPK phosphorylation was reduced in wild-type mice following HFD, but such effects were attenuated in IL-6 KO heart (Fig. 6D).

HFD increased STAT3 phosphorylation in heart, which is consistent with enhanced inflammation in diet-induced obese heart (Fig. 7A and B). Improved myocardial glucose

metabolism in HFD-fed IL-6 KO mice was associated with significant reductions in STAT3 phosphorylation, macrophages, and SOCS3 levels in these mice as compared with HFD-fed wild-type mice (Fig. 7B–D). These results demonstrate that IL-6 deficiency attenuates diet-induced cardiac inflammation and increases myocardial glucose metabolism, supporting the deleterious role of IL-6 in obese heart.

Acute lipid infusion causes cardiac inflammation. Our findings indicate that inflammation plays an important role in obesity-associated alterations in myocardial glucose metabolism. Obesity affects peripheral glucose metabolism through diverse mechanisms, including alterations in adipose secretion of fatty acids, hormones, and cytokines (27–30). In this regard, we hypothesized that fatty acids may trigger cardiac inflammation and alter glucose metabolism. Lipid emulsion plus heparin were intravenously infused for 5 h to raise circulating fatty acids levels in conscious C57BL/6 mice. Plasma FFA levels were raised by 3.5-fold over the glycerol-infused control groups (Fig. 8A), and heart samples were taken at the end of experiments. Acute lipid infusion induced cardiac inflammation, and local levels of IL-6 and TNF- α were increased by 1.5- to 2-fold in the heart (Fig. 8B and C). Local macrophage levels were also elevated by threefold following lipid infusion (Fig. 8D). We measured myocardial expression of CCR2, which binds the monocyte chemoattractant protein (MCP)-1 and regulates macrophage recruitment (31,32). CCR2 expression was elevated by 70% following lipid

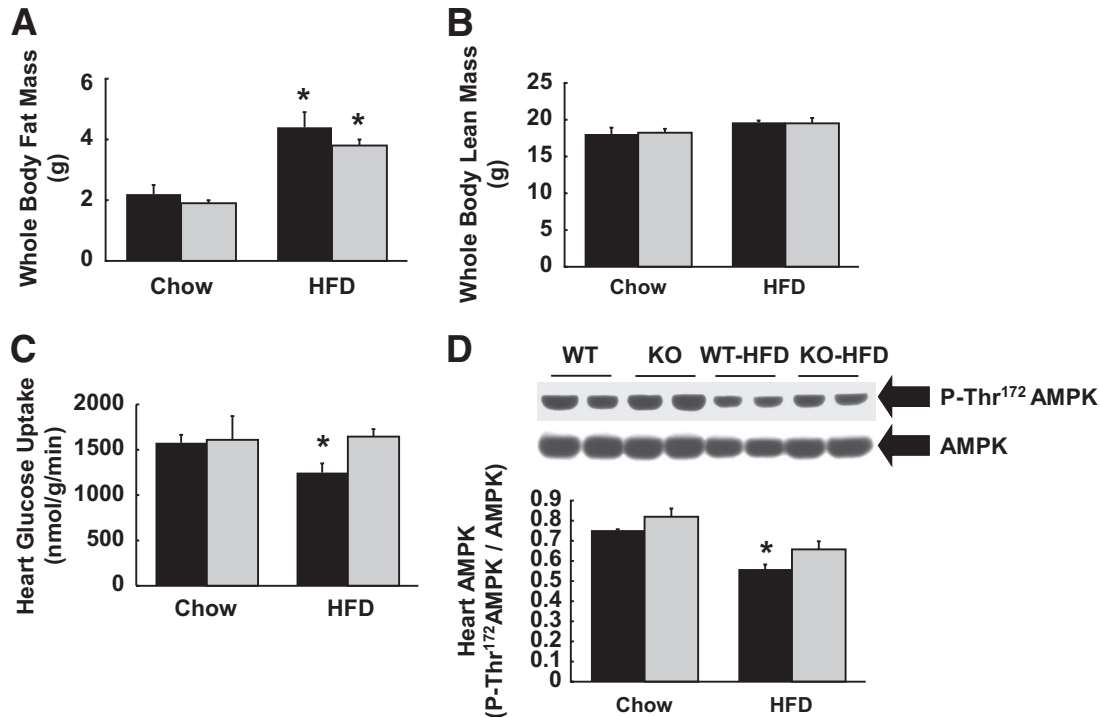


FIG. 6. IL-6 KO mice show improved myocardial glucose metabolism following HFD. Hyperinsulinemic-euglycemic clamps were performed in IL-6 KO and wild-type littermates (WT) following 3 weeks of standard (chow) diet or HFD, which began immediately after weaning in order to match whole-body adiposity in these mice. **A:** Whole-body fat mass was similarly elevated in IL-6 KO and wild-type mice following HFD. ■, Wild type; □, IL-6 KO. **B:** Whole-body lean mass was not different among groups. **C:** Insulin-stimulated glucose uptake was reduced in wild-type heart following HFD but remained normal in IL-6 KO heart. **D:** Thr¹⁷² phosphorylation of AMPK normalized to total AMPK protein levels was reduced in wild-type heart following HFD, but this effect was attenuated in IL-6 KO heart. Values are means \pm SE for four to seven mice in each experimental group. * $P < 0.05$ vs. wild-type mice.

infusion (Fig. 8E), and this was associated with increased levels of MyD88 in heart (Fig. 8F), supporting the role of TLR4 signaling in lipid-induced cardiac inflammation. Elevated levels of local cytokines in response to fatty acids tended to increase myocardial SOCS3 levels (0.101 ± 0.028 vs. 0.057 ± 0.016 in controls; $P = 0.16$) (Fig. 8G). Acute lipid infusion further reduced total AMPK protein and AMPK phosphorylation (Thr¹⁷²) levels in heart (Fig. 8H and D). These data are consistent with the role of inflammation in the regulation of myocardial AMPK. Overall, our results indicate that fatty acids act as nutrient stress that mediates obesity-induced cardiac inflammation and alterations in myocardial glucose metabolism.

DISCUSSION

Circulating levels of inflammatory cytokines are elevated in obese diabetic subjects, and the notion that type 2 diabetes has an inflammatory component is being widely accepted (9,33). Recent reports (8,11,34,35) indicate that obesity is associated with increased macrophage infiltration in adipose tissue and elevated adipocyte expression of MCP-1 and macrophage inflammatory protein-1 α . IL-6 and TNF- α , derived from macrophages and adipocytes, alter glucose metabolism in insulin-sensitive organs (14,21,26). Mice with adipocyte-specific overexpression of MCP-1 develop insulin resistance associated with increased macrophage infiltration in adipose tissue (34). Additionally, CCR2 binds to MCP-1 and regulates macrophage recruitment, and CCR2 KO mice show increased insulin sensitivity with reduced macrophage level in adipose tissue (32). While the effects of obesity on adipose inflammation are

well established, whether obesity causes inflammation in other organs remains poorly understood.

In this study, we report for the first time that diet-induced obesity causes inflammation and increases macrophage infiltration in heart. Similar to the effects in adipose tissue, diet-induced inflammatory response was associated with blunted myocardial glucose metabolism. TNF- α -induced insulin resistance in skeletal muscle was recently shown to involve transcriptional upregulation of protein phosphatase 2C and suppression of AMPK (15). Interestingly, plasma IL-6 and TNF- α levels were elevated in our diet-induced obese mice, and the cardiac inflammatory response was associated with significant reductions in AMPK phosphorylation. These results suggest that local macrophages and cytokines may be responsible for suppressing myocardial AMPK and downregulating glucose metabolism in heart. Since IL-6 was shown to alter glucose metabolism in peripheral organs (21,26), we examined the effects of acute IL-6 infusion on cardiac metabolism. IL-6 infusion markedly reduced basal myocardial glucose uptake, and this was associated with dramatic reductions in AMPK protein and phosphorylation levels in heart. IL-6 infusion also decreased IRS-1 tyrosine phosphorylation and insulin-stimulated glucose uptake in heart. These results support the notion that IL-6, at least in part, is responsible for diet-induced reductions in myocardial AMPK and glucose metabolism in mice. Acute IL-6 infusion caused a more dramatic reduction in total AMPK protein levels in heart as compared with chronic HFD, which may be due to elevated leptin levels associated with HFD-induced obesity. Furthermore, a recent study from Miller et al. (36) showed that macrophage migration

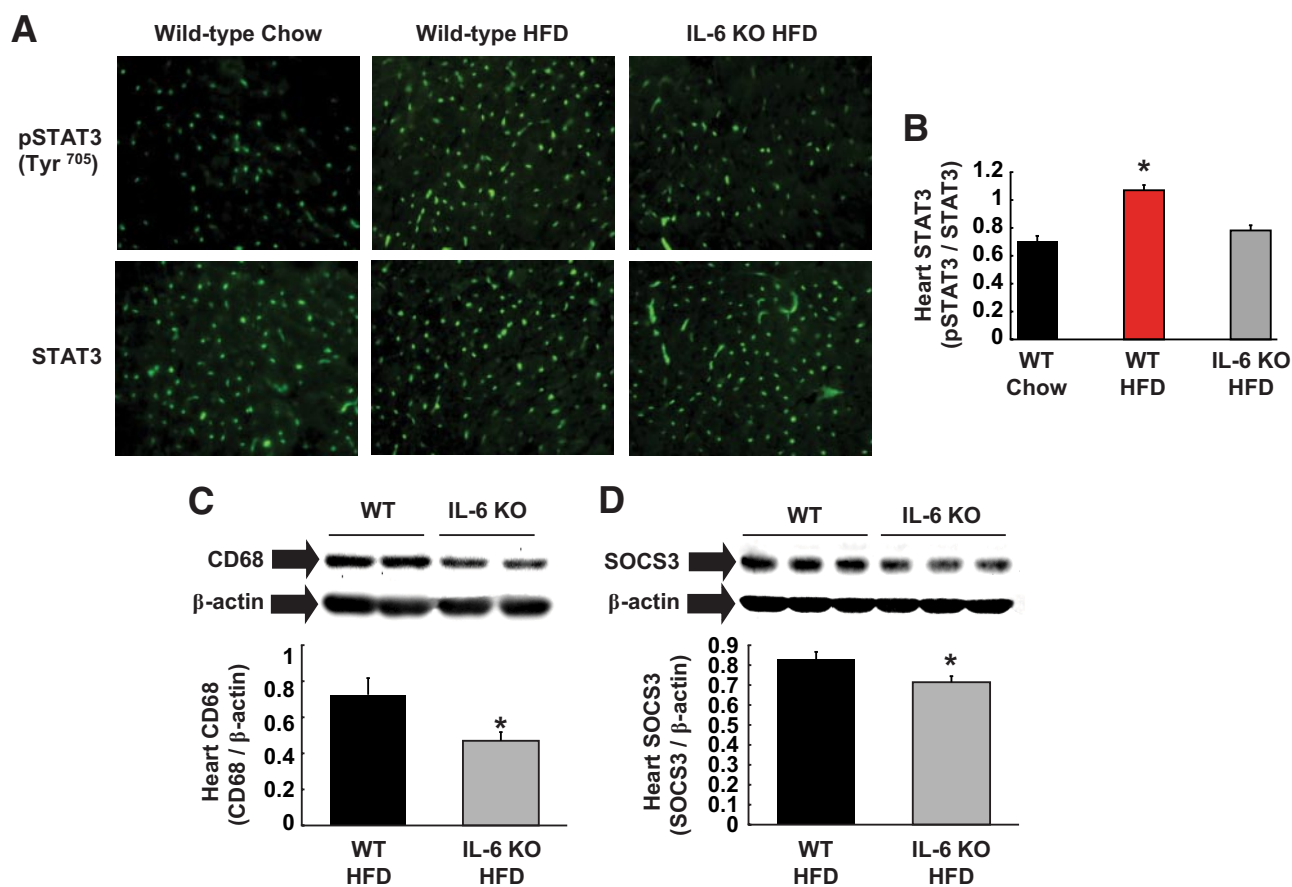


FIG. 7. IL-6 deletion attenuates diet-induced inflammatory response in heart. **A:** Immunofluorescence staining specific for Tyr⁷⁰⁵ phosphorylation of STAT3 was increased in wild-type (WT) heart but not in IL-6 KO heart following HFD without changes in total STAT3 levels. **B:** Quantification of phospho-STAT3 normalized to total STAT3 protein levels. **C:** Macrophage-specific CD68 levels normalized to β -actin in heart were lower in HFD-fed IL-6 KO mice. **D:** SOCS3 protein levels normalized to β -actin were reduced in IL-6 KO heart following HFD. Values are means \pm SE for four to seven mice in each experimental group. * $P < 0.05$ vs. wild-type mice. (A high-quality color digital representation of this figure is available in the online issue.)

inhibitory factor (MIF) stimulates AMPK in ischemic heart. It is unclear why MIF, which is an upstream regulator of inflammation, stimulates AMPK under ischemia, but obesity-associated inflammation suppresses AMPK in normal heart. More studies are clearly needed to determine whether this is associated with dose-dependent effects of MIF or in vivo versus in vitro effects of inflammation.

If IL-6 mediates diet-induced defects in cardiac glucose metabolism, mice lacking IL-6 may be protected from the deleterious effects of HFD. Surprisingly, IL-6 KO mice were previously found to be glucose intolerant and developed mature-onset obesity (37). However, glucose intolerance may be due to obesity, and not necessarily due to IL-6 deficiency, in IL-6 KO mice (38). Therefore, we designed a study to match the diet-induced adiposity by feeding an HFD to young IL-6 KO and wild-type mice, shortly after weaning, for 3 weeks. We have previously shown that myocardial glucose metabolism was reduced following 3 weeks of HFD in C57BL/6 mice (7). While HFD reduced myocardial glucose metabolism and AMPK phosphorylation in wild-type heart, IL-6 KO mice showed a partial protection from diet-induced defects in myocardial glucose uptake and AMPK. IL-6 deletion also attenuated and reduced myocardial levels of STAT3, CD68, and SOCS3 following HFD. Taken together, these data indicate that IL-6 plays an important role in regulating cardiac inflammation and glucose metabolism in diet-induced obesity.

The role of IL-6 in insulin resistance is controversial (19). We have previously shown that IL-6 suppresses muscle insulin signaling and glucose metabolism in mice (21). In contrast, Carey et al. (39) showed that IL-6 increases AMPK activity and glucose uptake in L6 myotubes. Additionally, Geiger et al. (40) demonstrated that IL-6 increases AMPK and insulin sensitivity only at superphysiological levels in rat skeletal muscle. Exercise has also been shown to increase IL-6 and SOCS3 gene expression in rat skeletal muscle (41), suggesting that IL-6 may impart differential effects under exercise condition (42). Although the role of IL-6 in muscle insulin action remains debatable, the metabolic effects of IL-6 in liver and adipose tissue are consistent and well established. IL-6 was shown to cause insulin resistance and alter insulin signaling in liver and adipocytes (17,18,26). Intracellular IL-6 signaling involves the tyrosine phosphorylation gp130 and activation of STAT3, which leads to the expression of SOCS3 (43). Previous studies (18,44–46) using isolated adipocytes and hepatocytes have shown that IL-6 downregulates insulin signaling by increasing SOCS3 that targets IRS-1 to ubiquitin-mediated degradation or blocks insulin receptor tyrosine phosphorylation. In the current study, HFD or IL-6 infusion also elevated SOCS3 expression in heart. In contrast, HFD-fed IL-6 KO mice showed lower SOCS3 levels in heart as compared with the HFD-fed wild-type mice. Furthermore, our findings that SOCS3 coimmuno-

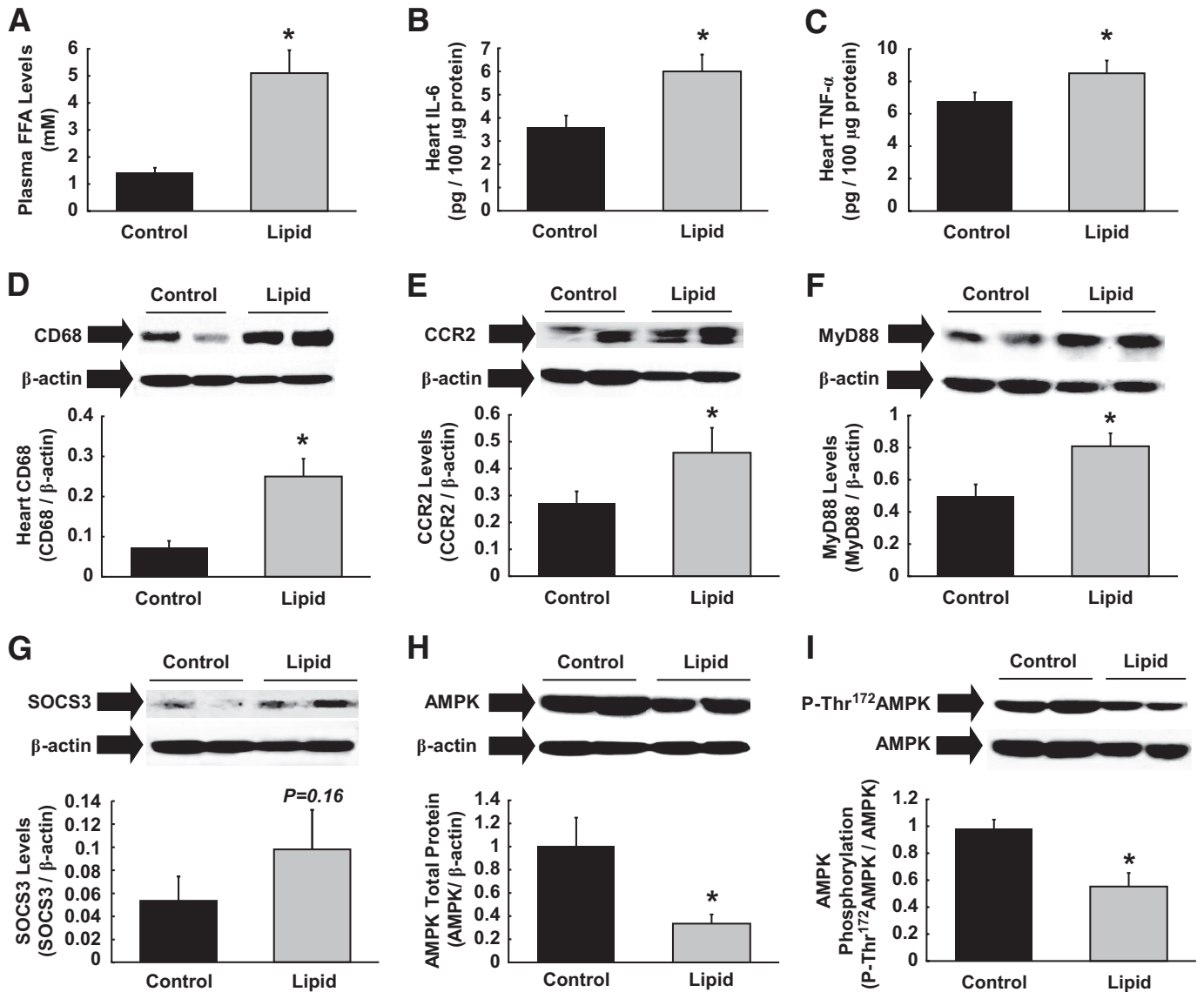


FIG. 8. Acute lipid infusion induces inflammation and suppresses AMPK in heart. Intralipid emulsion plus heparin or glycerol (control) were intravenously infused for 5 h in C57BL/6 mice, and heart samples were taken for analysis. *A*: Plasma FFA levels were increased by 3.5-fold following lipid infusion. *B* and *C*: Local IL-6 and TNF- α levels in heart were elevated in lipid-infused mice. *D–F*: Acute lipid infusion increased inflammation and macrophage-specific CD68, CCR2, and MyD88 levels in heart. All proteins were normalized to β -actin. *G*: Myocardial SOCS3 levels normalized to β -actin tended to be higher following lipid infusion. *H* and *I*: Total AMPK protein levels normalized to β -actin and Thr¹⁷²-phosphorylation of AMPK normalized to total AMPK protein levels were reduced in heart following lipid infusion. Values are means \pm SE for 6–11 mice in each experiment. * $P < 0.05$ vs. control.

precipitates with AMPK raises a possibility that IL-6–induced SOCS3 may target AMPK for ubiquitin-mediated degradation, similar to the established effects of SOCS3 on IRS proteins. However, we acknowledge the preliminary nature of these data due to limited antibodies used in the current study, and more studies are clearly needed to understand the possible regulation of AMPK by SOCS3. Nonetheless, our findings implicate that IL-6 modulates cardiac glucose metabolism possibly via STAT3/SOCS3-mediated downregulation of AMPK and insulin signaling in heart.

How does diet-induced obesity activate inflammation in heart? TLR4 was recently identified to bind to fatty acids and regulate lipid-mediated activation of inflammation and genes that encode inflammatory cytokines, such as TNF- α and IL-6 (24,25). Since high-fat feeding increased myocardial levels of TLR4 and MyD88, we examined the role of

fatty acids in diet-induced cardiac inflammation. Surprisingly, acute lipid infusion for 5 h, which raised circulating fatty acids, promoted dramatic inflammatory and metabolic events resembling the effects of high-fat feeding or IL-6 infusion. In this regard, acute lipid infusion markedly raised local macrophage, CCR2, MyD88, and cytokine levels in heart. Lipid-induced cardiac inflammation was associated with increased SOCS3 expression and profound reductions in AMPK protein and phosphorylation levels in heart. These results suggest that fatty acids may act as a nutrient stress that signals cardiac inflammation and downregulates myocardial glucose metabolism.

In conclusion, our findings identify a novel role of inflammation in obesity-associated alterations in myocardial glucose metabolism and insulin resistance. Fatty acids may act as a nutrient stress that induces inflammation in heart by activating TLR4 signaling and increasing local

macrophage and cytokine levels. IL-6 downregulates myocardial glucose metabolism and causes insulin resistance by suppressing AMPK and insulin signaling in heart. The underlying mechanism involves an IL-6-induced increase in SOCS3 and SOCS3-mediated degradation of IRS-1 and possibly AMPK in heart. Since AMPK activation and glucose metabolism provide an important source of energy for heart under stress conditions, such as ischemia, obesity-induced cardiac inflammation and defects in myocardial glucose metabolism may play an important role in the pathogenesis of diabetic heart.

ACKNOWLEDGMENTS

This study was supported by grants from the U.S. Public Health Service (R01-DK80756 to J.K.K.), the American Diabetes Association (1-04-RA-47 and 7-07-RA-80 to J.K.K.), the American Heart Association (0855492D to J.K.K.), and a grant from the Pennsylvania Department of Health using Tobacco Settlement Funds (to J.K.K.).

No potential conflicts of interest relevant to this article were reported.

Parts of this study were presented in abstract form at the 68th Scientific Sessions of the American Diabetes Association, San Francisco, California, 6–10 June 2008, and at the American Heart Association's Scientific Sessions, New Orleans, Louisiana, 8–12 November 2008.

REFERENCES

- Grundy SM, Benjamin IJ, Burke GL, Chait A, Eckel RH, Howard BV, Mitch W, Smith SC, Sowers JR. Diabetes and cardiovascular disease: a statement for healthcare professionals from the American Heart Association. *Circulation* 1999;100:1134–1146
- Rodrigues B, McNeill JH. The diabetic heart: metabolic causes for the development of a cardiomyopathy. *Cardiovascular Res* 1992;26:913–922
- Taegtmeier H, Passmore JM. Defective energy metabolism of the heart in diabetes. *Lancet* 1985;1:139–141
- Kolter T, Uphues I, Eckel J. Molecular analysis of insulin resistance in isolated ventricular cardiomyocytes of obese Zucker rats. *Am J Physiol* 1997;273:E59–E67
- Ohtake T, Yokoyama I, Watanabe Y, Momose T, Serezawa T, Nishikawa J, Sasaki Y. Myocardial glucose metabolism in noninsulin-dependent diabetes mellitus patients evaluated by FDG-PET. *J Nucl Med* 1995;36:456–463
- Lopaschuk GD. Abnormal mechanical function in diabetes: relationship to altered myocardial carbohydrates/lipid metabolism. *Coronary Artery Dis* 1996;7:116–123
- Park S-Y, Cho Y-R, Kim H-J, Higashimori T, Danton C, Lee M-K, Dey A, Rothermel B, Kim Y-B, Kalinowski A, Russell KS, Kim JK. Unraveling the temporal pattern of diet-induced insulin resistance in individual organs and cardiac dysfunction in C57BL/6 mice. *Diabetes* 2005;54:3530–3540
- Chen H. Cellular inflammatory responses: novel insights for obesity and insulin resistance. *Pharmacological Res* 2006;53:469–477
- Wellen KF, Hotamisligil GS. Inflammation, stress, diabetes. *J Clin Invest* 2005;115:1111–1119
- Di Gregorio GB, Yao-Borengasser A, Rasouli N, Varma V, Lu T, Miles LM, Ranganathan G, Peterson CA, McGehee RE, Kern PA. Expression of CD68 and macrophage chemoattractant protein-1 genes in human adipose and muscle tissues. *Diabetes* 2005;54:2305–2313
- Lumeng CN, Deyoung SM, Saltiel AR. Macrophages block insulin action in adipocytes by altering expression of signaling and glucose transport proteins. *Am J Physiol* 2007;292:E166–E174
- Permana PA, Menge C, Reaven PD. Macrophage-secreted factors induce adipocyte inflammation and insulin resistance. *Biochem Biophys Res Comm* 2006;341:507–514
- Xu H, Barnes GT, Yang Q, Tan G, Yang D, Chou CJ, Sole J, Nichols A, Ross JS, Tartaglia LA, Chen H. Chronic inflammation in fat plays a crucial role in the development of obesity-related insulin resistance. *J Clin Invest* 2003;112:1821–1830
- Hotamisligil GS, Shargill NS, Spiegelman BM. Adipose expression of tumor necrosis factor- α : direct role in obesity-linked insulin resistance. *Science* 1993;259:87–91
- Steinberg GR, Michell BJ, van Denderen BJW, Watt MJ, Carey AL, Fam BC, Andrikopoulos S, Proietto J, Gorgun CZ, Carling D, Hotamisligil GS, Febbraio MA, Kay TW, Kemp BE. Tumor necrosis factor α -induced skeletal muscle insulin resistance involves suppression of AMP-kinase signaling. *Cell Metab* 2006;4:465–474
- Kern PA, Ranganathan S, Li C, Wood L, Ranganathan G. Adipose tissue tumor necrosis factor and interleukin-6 expression in human obesity and insulin resistance. *Am J Physiol* 2001;280:E745–E751
- Senn JJ, Klover PJ, Nowak IA, Mooney RA. Interleukin-6 induces cellular insulin resistance in hepatocytes. *Diabetes* 2002;51:3391–3399
- Shi H, Tzameli I, Bjorbaek C, Flier JS. Suppressor of cytokine signaling 3 is a physiological regulator of adipocyte insulin signaling. *J Biol Chem* 2004;279:34733–34740
- Pedersen BK, Febbraio MA, Mooney RA. Interleukin-6 does/does not have a beneficial role in insulin sensitivity and glucose homeostasis. *J Appl Physiol* 2007;102:814–816
- Park S-Y, Cho Y-R, Finck BN, Kim H-J, Higashimori T, Hong E-G, Lee M-K, Danton C, Deshmukh S, Cline GW, Wu JJ, Bennett AM, Rothermel B, Kalinowski A, Russell KS, Kim Y-B, Kelly DP, Kim JK. Cardiac-specific overexpression of PPAR α causes insulin resistance in heart and liver. *Diabetes* 2005;54:2514–2524
- Kim HJ, Higashimori T, Park SY, Choi H, Dong J, Kim YJ, Noh HL, Cho YR, Cline G, Kim YB, Kim JK. Differential effects of interleukin-6 and 10 on skeletal muscle and liver insulin action in vivo. *Diabetes* 2004;53:1060–1067
- Stanley WC, Lopaschuk GD, McCormack JG. Regulation of energy substrate metabolism in the diabetic heart. *Cardiovasc Res* 1997;34:25–33
- Young LH, Li J, Baron SJ, Russell RR. AMP-activated protein kinase: a key stress signaling pathway in the heart. *Trends Cardiovasc Med* 2005;15:110–118
- Shi H, KoKoeva MV, Inouye K, Tzameli I, Yin H, Flier JS. TLR4 links innate immunity and fatty acid-induced insulin resistance. *J Clin Invest* 2006;116:3015–3025
- Kim JK. Fat uses a TOLL-road to connect inflammation and diabetes. *Cell Metab* 2006;4:417–418
- Klover PJ, Zimmers TA, Koniaris LG, Mooney RA. Chronic exposure to interleukin-6 causes hepatic insulin resistance in mice. *Diabetes* 2003;52:2784–2789
- Boden G, Shulman GI. Free fatty acids in obesity and type 2 diabetes: defining their role in the development of insulin resistance and beta-cell dysfunction. *Eur J Clin Invest* 2002;32:14–23
- Kadowaki T, Yamauchi T. Adiponectin and adiponectin receptors. *Endocr Rev* 2005;26:439–451
- Steppan CM, Bailey ST, Bhat S, Brown EJ, Banerjee RR, Wright CM, Patel HR, Ahima RS, Lazar MA. The hormone resistin links obesity to diabetes. *Nature* 2001;409:307–312
- Stratford S, Hoehn KL, Liu F, Summers SA. Regulation of insulin action by ceramide: dual mechanisms linking ceramide accumulation to the inhibition of Akt/protein kinase B. *J Biol Chem* 2004;279:36608–36615
- Kurihara T, Bravo R. Cloning and functional expression of mCCR2, a murine receptor for the C-C chemokines JE and FIC. *J Biol Chem* 1996;271:11603–11607
- Weisberg SP, Hunter D, Hubner R, Lemieux J, Slaymaker S, Vaddi K, Charo I, Leibel RL, Ferrante AW Jr. CCR2 modulates inflammatory and metabolic effects of high-fat feeding. *J Clin Invest* 2006;116:115–124
- Pickup JC, Chusney GD, Thomas SM, Burt D. Plasma interleukin-6, tumor necrosis factor α and blood cytokine production in type 2 diabetes. *Life Sci* 2000;67:291–300
- Kanda H, Tateya S, Tamori Y, Kokota K, Hiasa K-I, Kitazawa R, Kitazawa S, Miyachi H, Maeda S, Egashira K, Kasuga M. MCP-1 contributes to macrophage infiltration into adipose tissue, insulin resistance, and hepatic steatosis in obesity. *J Clin Invest* 2006;116:1494–1505
- Takahashi K, Mizuurai S, Araki H, Mashiko S, Ishihara A, Kanatani A, Itadani H, Kotani H. Adiposity elevates plasma MCP-1 levels leading to the increased CD11b-positive monocytes in mice. *J Biol Chem* 2003;278:46654–46660
- Miller EJ, Li J, Leng L, McDonald C, Atsumi T, Bucala R, Young LH. Macrophage migration inhibitory factor stimulates AMP-activated protein kinase in the ischaemic heart. *Nature* 2008;451:578–583
- Wallenius V, Wallenius K, Ahren B, Rudling M, Carlsten H, Dickson SL, Ohlsson C, Jansson J-O. Interleukin-6-deficient mice develop mature-onset obesity. *Nat Med* 2002;8:75–79
- Di Gregorio GB, Hensley L, Lu T, Ranganathan G, Kern PA. Lipid and carbohydrate metabolism in mice with a targeted mutation in the IL-6 gene: absence of development of age-related obesity. *Am J Physiol* 2004;287:E182–E187
- Carey AL, Steinberg GR, Macaulay SL, Thomas WG, Holmes AG, Ramm G,

- Prelovsek O, Hohnen-Behrens C, Watt MJ, James DE, Kemp BE, Pedersen BK, Febbraio MA. Interleukin-6 increases insulin-stimulated glucose disposal in humans and glucose uptake and fatty acid oxidation in vitro via AMP-activated protein kinase. *Diabetes* 2006;55:2688–2697
40. Geiger PC, Hancock C, Wright DC, Han D-H, Holloszy JO. IL-6 increases muscle insulin sensitivity only at superphysiological levels. *Am J Physiol* 2007;292:E1842–E1846
41. Spangenburg EE, Brown DA, Johnson MS, Moore RL. Exercise increases SOCS-3 expression in rat skeletal muscle: potential relationship to IL-6 expression. *J Physiol* 2006;572:839–848
42. Febbraio MA, Pedersen BK. Muscle derived interleukin-6: mechanisms for activation and possible biological roles. *FASEB J* 2002;16:1335–1347
43. Hirano T, Ishihara K, Hibi M. Roles of STAT3 in mediating the cell growth, differentiation and survival signals relayed through the IL-6 family of cytokine receptors. *Oncogene* 2000;19:2548–2556
44. Emanuelli B, Peraldi P, Filloux C, Sawka-Verhelle D, Hilton D, Van Obberghen E. SOCS-3 is an insulin-induced negative regulator of insulin signaling. *J Biol Chem* 2000;275:15985–15991
45. Rui L, Yuan M, Frantz D, Shoelson S, White MF. SOCS-1 and SOCS-3 block insulin signaling by ubiquitin-mediated degradation of IRS1 and IRS2. *J Biol Chem* 2002;277:42394–42398
46. Senn JJ, Klover PJ, Nowak IA, Zimmers TA, Koniaris LG, Furlanetto RW, Mooney RA. Suppressor of cytokine-signaling-3 (SOCS-3), a potential mediator of interleukin-6-dependent insulin resistance in hepatocytes. *J Biol Chem* 2003;278:13740–13746